



# A GPU-accelerated Branch-and-Bound Algorithm for the Flow-Shop Scheduling Problem

Nouredine Melab, Imen Chakroun, Mohand Mezmaz, Daniel Tuyttens

## ► To cite this version:

Nouredine Melab, Imen Chakroun, Mohand Mezmaz, Daniel Tuyttens. A GPU-accelerated Branch-and-Bound Algorithm for the Flow-Shop Scheduling Problem. 14th IEEE International Conference on Cluster Computing, Cluster'12, Sep 2012, Beijin, China. hal-00723736

**HAL Id: hal-00723736**

**<https://inria.hal.science/hal-00723736>**

Submitted on 18 Aug 2012

**HAL** is a multi-disciplinary open access archive for the deposit and dissemination of scientific research documents, whether they are published or not. The documents may come from teaching and research institutions in France or abroad, or from public or private research centers.

L'archive ouverte pluridisciplinaire **HAL**, est destinée au dépôt et à la diffusion de documents scientifiques de niveau recherche, publiés ou non, émanant des établissements d'enseignement et de recherche français ou étrangers, des laboratoires publics ou privés.

# A GPU-accelerated Branch-and-Bound Algorithm for the Flow-Shop Scheduling Problem

N. Melab<sup>\*</sup>, I. Chakroun<sup>\*</sup>, M. Mezmaz<sup>\*\*</sup> and D. Tuytens<sup>\*\*</sup>

<sup>\*</sup> Université Lille 1, LIFL/UMR CNRS 8022

59655 - Villeneuve d'Ascq cedex - France

Email: {nouredine.melab, imen.chakroun}@lfl.fr

Mathematics and OR Department, University of Mons, Belgium

Email: {mohand.mezmaz,daniel.tuytens}@umons.ac.be

**Abstract**—Branch-and-Bound (B&B) algorithms are time-intensive tree-based exploration methods for solving to optimality combinatorial optimization problems. In this paper, we investigate the use of GPU computing as a major complementary way to speed up those methods. The focus is put on the bounding mechanism of B&B algorithms, which is the most time consuming part of their exploration process. We propose a parallel B&B algorithm based on a GPU-accelerated bounding model. The proposed approach concentrate on optimizing data access management to further improve the performance of the bounding mechanism which uses large and intermediate data sets that do not completely fit in GPU memory. Extensive experiments of the contribution have been carried out on well-known FSP benchmarks using an Nvidia Tesla C2050 GPU card. We compared the obtained performances to a single and a multi-threaded CPU-based execution. Accelerations up to  $\times 100$  are achieved for large problem instances.

**Index Terms**—Massively Parallel Computing, GPU Computing, Branch-and-Bound Algorithms, Lower Bounding, Flow-Shop Scheduling.

## I. INTRODUCTION

Combinatorial optimization problems<sup>1</sup> are NP-hard and CPU-time intensive in practice. Branch-and-Bound (B&B) algorithms are efficient methods for solving to optimality those problems. Their execution consists in exploring a search space by dynamically building a tree whose root node is the original problem, the intermediate nodes are sub-problems, and the leaves are potential solution(s). B&B proceeds in several iterations during which the best solution found so far (upper bound) is progressively improved. During the exploration, a bounding mechanism, based on a lower bound function, is used to eliminate all the sub-problems (i.e. cut their corresponding sub-trees) that are not likely to lead to optimal solutions. Such powerful mechanism allows one to reduce significantly the size of the explored search space and thus its exploration time cost.

However, even if such mechanism is highly efficient it is not sufficient to deal with large size problem instances. Over the last decades, parallel computing has emerged as an

attractive way to deal with larger instances. The design and implementation of parallel B&B is strongly influenced by the computing platform. Many contributions have been proposed for the design and implementation of parallel B&B methods using Massively Parallel Processors (MPP) [8], Networks or Clusters of Workstations (NOWs or COWs) [7] and Shared Memory or SMP machines [9]. In this paper, we investigate the design of B&B algorithms on Graphics Processing Units (GPU). In combinatorial optimization, GPU computing is successfully used for meta-heuristics (near-optimal methods) [14] but not yet for B&B exact methods.

Most of existing parallel B&B algorithms are based on the parallel exploration of the search tree. Such parallel model is not suited to GPUs because the explored search tree is highly irregular. The best parallel model for B&B on GPU is the parallel evaluation of the lower bound function (thread kernel) on pools of sub-problems (parallel bounding). Such model must be rethought at design as well as at implementation level taking into account at the same time the characteristics of GPU accelerators and those of the lower bound computation function. On the one hand, a GPU is a many-core co-processor device that provides a hierarchy of memories having different sizes and access latencies making data placement and sharing challenging. On the other hand, the lower bound computation function is generally problem-dependent. In this paper, the focus is on the Flow-Shop scheduling permutation Problem (FSP) (see Section II-B). The lower bound function used in this work for FSP is that proposed in [5] for two machines and generalized in [3] to more than two machines. The implementation of such function makes use of six data structures of different sizes and access frequencies making data placement on GPU challenging.

Preliminary experiments we have carried out on some Taillard's FSP instances [6] have shown that the time spent by B&B evaluating the lower bounds of the examined sub-problems is on average around 98.5% of its total execution time. Such result illustrates the potential benefit of parallelizing the bounding operation. The major contribution of this paper consists in revisiting B&B to allow efficient solving of large FSP instances on GPU. Having in mind the characteristics of both the lower bound function and the GPU

<sup>1</sup>An optimization problem consists in minimizing or maximizing a cost function. Without loss of generality, in this paper the minimization case is considered.

device mentioned above, the challenge is to define a new approach for optimal mapping of the data structures of the lower bound function on the hierarchy of memories provided in the GPU device. A careful analysis is required of both the data structures (size and access frequency) and the GPU memories (size and access latency).

The remainder of the paper is organized as follows: Section II presents the B&B algorithm applied to the permutation FSP, the associated lower bound used in this paper, and its implementation and complexity analysis. In Section III, we describe our GPU-based proposed approach for B&B applied to FSP. Details are given on the parallel approach and memory access optimization. In Section IV, we report experimental results demonstrating the efficiency of our approach. In Section V we compare the performance of the proposed approach to a multi-threaded CPU version of the B&B. Finally, some conclusions and perspectives of this work are drawn in Section VI.

## II. B&B AND LOWER BOUND FOR THE PERMUTATION FSP

### A. Parallel B&B algorithms

Branch-and-Bound (B&B) algorithms are based on an implicit enumeration of the solutions composing the search space associated to the problem to be tackled. The search space is explored by dynamically building a tree whose root node designates the original problem. The construction of the B&B tree and its exploration are performed using four operators: *branching*, *bounding*, *selection* and *elimination*. The algorithm proceeds in several iterations during which the best solution found so far (upper bound) is progressively improved. The generated and not yet examined sub-problems are kept into a list initialized to the original problem. At each iteration, a sub-problem is selected from this list, according to some strategy (depth-first, best-first, ...), using the *selection operator*. The *branching operator* performs its decomposition into other sub-problems. The *bounding operator* calculates a lower bound of each generated sub-problem. Each sub-problem having a lower bound greater than the upper bound is eliminated using the *elimination operator*, this means that it will not be decomposed.

Existing parallel B&B algorithms are based on three parallel models proposed in [1]: parallel application of the operators on the generated sub-problems (Type 1), parallel building and exploration of a B&B tree (Type 2), and parallel (cooperative or independent) building and exploration of several B&B trees (Type 3). We have later revisited these parallel approaches for large-scale computational grids [13] using Type 2 parallel model. Grid computing provides an impressive computing power to solve challenging instances in combinatorial optimization [11]. However, computational grids providing a huge amount of resources are not easily available and accessible for any user. Recently, Graphics Processing Units (GPU accelerators) have emerged as a new popular support for massively parallel computing. Such resources supply a great computing power, are energy-efficient and unlike grids they are highly available every where: laptops, desktops, clusters, etc. In the

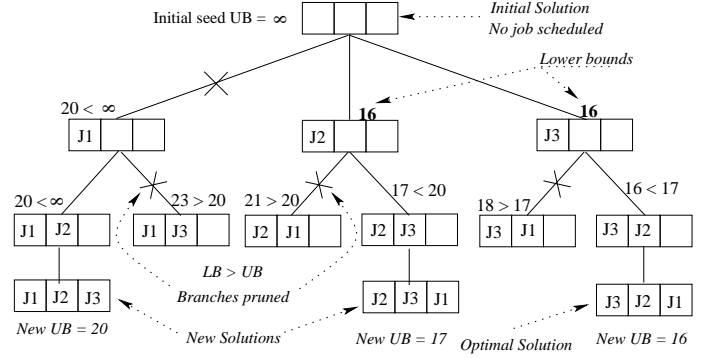


Fig. 1. The search tree generated and explored by a B&B algorithm for solving an FSP with 3 jobs. Nodes with a lower bound (LB) greater (resp. lower or equal) than the upper bound (UB) are pruned (resp. decomposed or branched).

following, we revisit the Type 1 parallel model on GPU for solving Flow-Shop problems.

### B. B&B for the permutation FSP

The general FSP [3] consists in scheduling a pool of  $n$  jobs on a set of  $m$  machines such that each of the jobs  $J_1, J_2, \dots, J_n$  has to be processed on the machines  $M_1, M_2, \dots, M_m$  in that order. Job  $J_i$  ( $i = 1, 2, \dots, n$ ) consists therefore of a sequence of  $m$  operations  $O_{i1}, O_{i2}, \dots, O_{im}$ ;  $O_{ik}$  being the processing of  $J_i$  on  $M_k$  during an uninterrupted processing time  $p_{ik}$ .  $M_k$  ( $k = 1, 2, \dots, m$ ) can handle at most one job at a time. The objective is to find a processing order on each  $M_k$  such that the time (makespan) required to complete all jobs is minimized. If the problem is restricted to the minimization over all permutation schedules, meaning with the same processing order on each machine, the resulting problem is called the permutation Flow-Shop problem, which is the focus of this work. In the remainder of this paper, FSP designates a permutation FSP.

For  $m = 2$ , an optimal schedule can be found in  $O(n \log n)$  steps using Johnson's algorithm [5]. For  $m \geq 3$ , the problem has been shown to be NP-hard [4]. Due to such complexity the enumerative solution approach provided in B&B algorithms is well-suited to solve the problem to optimality. As illustrated (for  $n = 3$ ) in Figure 1, the B&B enumeration scheme is based on a search tree whose root node contains the original problem (empty schedule).

The decomposition of this problem generates  $n$  sons, each of them designates a sub-problem. The son number  $i$  represents the sub-problem in which job  $J_i$  is scheduled first on all machines. The recursive application of the decomposition operator on the generated sub-problems allows to develop the search tree. The number of potential schedules (permutations) is  $n!$ , which is highly exorbitant for large problem instances such as  $200 \times 20$  ( $200!$  schedules!) Taillard's ones [6]. There are two major powerful ways to speed up the exploration of large search trees. The first way consists in using an efficient bounding operator. Applied to a sub-problem, such operator

associates a value to its corresponding tree node using a lower bound function. As illustrated in Figure 1, the sub-problem is not decomposed (and its tree node is pruned) if its lower bound value is greater than the cost of the best schedule found so far (called the upper bound) during the exploration of the search tree. The second way is to use massively parallel computing based on the three parallelism types presented in Section II-A. We recall that the focus of this paper is only on *Type 1* i.e. the parallel evaluation of the lower bound on a pool of sub-problems.

### C. Lower Bound for FSP

As quoted above, the objective (cost function) of FSP considered in this paper is the makespan  $C_{max}$ , which represents the completion time of the last scheduled job on the last machine. Given a sub-problem (partial schedule)  $\pi = \pi(1), \pi(2), \dots, \pi(l)$  indicating that  $J_{\pi(i)}$  occupies the  $i^{th}$  position on each machine for  $i = 1, \dots, l$ . The sub-problem consists to find the optimal schedule of the  $n-l$  remaining unscheduled jobs. Before solving such sub-problem, it is checked either or not the optimal solution of the original problem could be the optimal solution of this sub-problem. In other words, it is checked either the optimal solution of the original problem is probably in the sub-tree search space associated to that sub-problem or not. This is the role of the bounding operator which uses a lower bound function to prune nodes and the sub-trees they are root of. Indeed, if the lower bound value of the sub-problem is greater than the upper bound found so far the sub-problem is not decomposed/branched because it is sure that the optimal solution is not located in its sub-tree search space. This allows to significantly reduce the exploration time of the B&B tree. Therefore, the efficiency of a B&B algorithm depends strongly on the quality of its lower bound function. In this paper, we use the lower bound proposed by Lenstra *et al.* [3] for FSP, based on the Johnson's algorithm [5].

### D. Complexity analysis and implementation

For an efficient implementation of the lower bound LB algorithm, six data structures are required: the matrix  $PTM$  of the processing times of the jobs, the matrix of lags  $LM$ , the Johnson's matrix  $JM$ , the matrix  $RM$  of the earliest starting times of jobs, the matrix  $QM$  of their lowest latency times and the matrix  $MM$  containing the couples of machines. In the  $LB$  expression, the computation of the term  $P_{ja}^*(j, M_k, M_l)$  requires the calculation of the lag of each remaining job to be scheduled on the couple  $(M_k, M_l)$  of machines using its processing times on these machines (Johnson's rule with lags). Such computation is repeated for each couple  $(M_k, M_l)$  of machines with  $1 \leq k, l \leq m$  and  $k < l$ . To avoid the repetitive computation of the lags, they are computed once at the beginning of the algorithm and stored in the matrix  $LM$ . The dimension of  $LM$  is  $n \times \frac{m \times (m-1)}{2}$ , where  $n$  and  $m$  are respectively the number of jobs to be scheduled and  $m$  the number of machines.  $LM$  is accessed  $n' \times \frac{m \times (m-1)}{2}$  times,  $n'$  being the number of remaining jobs to be scheduled in the sub-problem for which

Matrix	Size	Number of accesses
PTM	$n \times m$	$n' \times m \times (m-1)$
LM	$n \times \frac{m \times (m-1)}{2}$	$n' \times \frac{m \times (m-1)}{2}$
JM	$n \times \frac{m \times (m-1)}{2}$	$n \times \frac{m \times (m-1)}{2}$
RM	$m$	$m \times (m-1)$
QM	$m$	$\frac{m \times (m-1)}{2}$
MM	$m \times (m-1)$	$m \times (m-1)$

TABLE I  
THE DIFFERENT DATA STRUCTURES OF THE  $LB$  ALGORITHM AND THEIR ASSOCIATED COMPLEXITIES IN MEMORY SIZE AND NUMBERS OF ACCESSES. THE PARAMETERS  $n$ ,  $m$  AND  $n'$  DESIGNATE RESP. THE TOTAL NUMBER OF JOBS, THE TOTAL NUMBER OF MACHINES AND THE NUMBER OF REMAINING JOBS TO BE SCHEDULED FOR THE SUB-PROBLEMS THE LOWER BOUND IS BEING COMPUTED.

```

(01) int computeLB(){
(02)   LB=maxInteger;
(03)   for (index=0;index<  $\frac{m \times (m-1)}{2}$ ;index++){
(04)     M1=MM[index][0];
(05)     M2=MM[index][1];
(06)     timeOnM1=  $\min_{0 \leq j \leq n}$  (RM[M1][j]);
(07)     timeOnM2=  $\min_{0 \leq j \leq n}$  (RM[M2][j]);2
(08)     for (i=0;i<n;i++){
(09)       job=JM[i][index];
(10)       if (job not yet scheduled){
(11)         timeOnM1=timeOnM1+PTM[job][M1];
(12)         if (timeOnM2>timeOnM1+LM[job][index])(*)
(13)           timeOnM2+=PTM[job][M2];
(14)         else
(15)           timeOnM2=timeOnM1+LM[job][index]+
(16)             PTM[job][M2];
(17)       }
(18)     }
(19)     timeOnM2+=  $\min_{0 \leq j \leq n}$  (QM[M2][j]);
(20)     LB=max(timeOnM2,LB);
(21)   }
(22) }
return LB;

```

Fig. 2. Pseudo-code implementing the LB function

the lower bound is being calculated. The processing times of all the jobs on all the machines are stored in the matrix  $PTM$ . This matrix has a dimension of  $n \times m$  and is accessed  $n' \times m \times (m-1)$  times.

Table I, is highly needed to understand the proposed data placement approach. The columns of Table I represent respectively the name of the data structure, its size and the number of times it is accessed. Figure 2 shows the pseudo-code implementing the  $LB$  lower bound function illustrating the access to the six data structures.

### III. GPU-BASED B&B FOR FSP - A NEW APPROACH

As said previously, the time complexity of the Johnson algorithm for two machines is  $O(n \cdot \log n)$ . Therefore, the



time complexity of the lower bound  $LB$  for  $m$  machines is  $O(m^2 \cdot n \cdot \log n)$ . The computation of the lower bound is consequently time intensive especially for problem instances for which  $m$  is high. In order to evaluate experimentally its CPU time cost, we have implemented this lower bound and experimented it using the most time-consuming Taillard's instances [6] i.e. having  $m = 20$ . The results show that the time spent by the B&B evaluating the lower bounds of the examined sub-problems is on average around 98.5% of its total execution time. Such result demonstrates that the bounding must be parallelized i.e. the  $LB$  lower bound function must be applied in parallel to each sub-problem composing the pool of sub-problems currently examined. In the following, we present a new GPU-based approach for the parallel evaluation of the lower bound in B&B algorithms. We first present the parallel GPU-based approach. Then, we show how our approach maps the different data structures on the memory hierarchy of the GPU device taking into account the characteristics of the data structures presented in Table I and those of the different GPU memories (size and access latency).

#### A. The GPU-based parallel evaluation of $LB$

The GPU-accelerated approach is based on the GPGPU (CUDA or OpenCL) parallel paradigm according to which the programmer writes a serial program that calls parallel kernels (simple functions or full programs). A kernel executes in parallel across a set of parallel threads. The programmer organizes these threads into a hierarchy of grids of thread blocks. A thread block is a set of concurrent threads that can cooperate through barrier synchronization and shared access to a memory space private to the block. A grid is a set of thread blocks that may be executed independently in parallel. When invoking a kernel, the programmer specifies the execution configuration. Such configuration includes the number of threads per block and the number of blocks making up the grid.

In our proposed GPU-based approach, the generation of the sub-problems (elimination, selection and branching operations) to be solved is performed on CPU and the evaluation of their lower bounds (bounding operation) is executed on the GPU device. As illustrated in Figure 3, the pool of sub-problems generated on CPU (and selected according to the well-know best-first strategy) is off-loaded to the GPU device to be evaluated by a pool of threads partitioned into blocks. Each thread applies the lower bound function (kernel) to one sub-problem. Once the evaluation is completed, the lower bound values of the different sub-problems are returned back to the CPU to be used by the elimination operator to decide either to be pruned or to be decomposed. The process is iterated until the exploration is completed and the optimal solution is found.

#### B. Data access optimization

During their execution, threads may access data from multiple memory spaces having different sizes and access latencies. At the thread-level, each thread has its own allocated registers

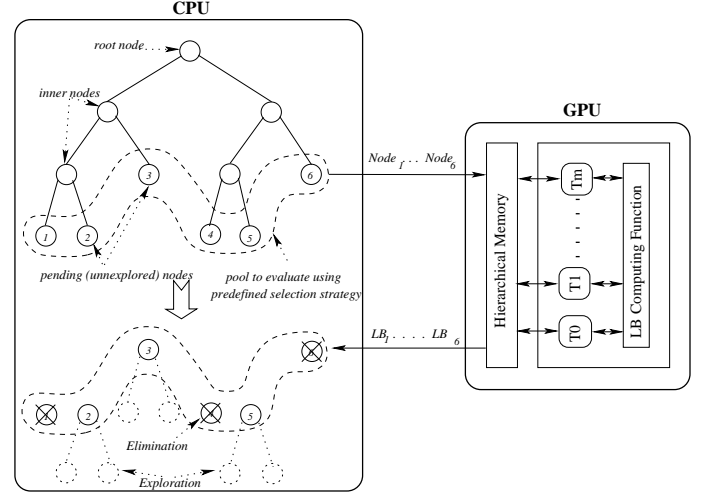


Fig. 3. GPU evaluation of sub-problems: generation on CPU and evaluation on GPU.

and a private local memory. CUDA [17] uses this local memory for thread-private variables that do not fit in the threads registers, as well as for stack frames and register spilling. At the thread block-level, each thread block has a shared memory visible to all its associated threads. At the grid-level, all threads have access to the same global memory. Texture and constant cached memories are two other memories accessible by all threads. The data access optimization challenge is to find the best mapping of the data structures of the application at hand (different sizes and access frequencies) and the GPU hierarchy of memories (different sizes and access latencies). For instance, the global memory is large in size but has a high access latency. On the contrary, shared memory is smaller in size but has a lower access latency.

For B&B applied to FSP, threads of the same block perform concurrent accesses to the six data structures of the problem when they execute the  $LB$  lower bound function. To optimize the performance of such application, the best mapping of the data structures is to copy them on the shared memory of the GPU device. However, for large problem instances all of the data structures do not fit into the shared memory which size is limited and depends on the GPU hardware configuration. The challenge is therefore to decide which data structure must be put in the shared memory to get the best performance. The answer is given in the next section according to the complexity analysis presented in Table I and the underlying GPU configuration of our experiments.

## IV. EXPERIMENTS

To evaluate the performance of our GPU-based B&B algorithm and parallel bounding approach, we have considered the largest Taillard's FSP benchmarks proposed in [6], except those with 500 jobs because they do not fit in the memory of the CPU. The different instances are designated by  $n \times m$ , where  $n$  and  $m$  represent respectively the number of jobs (between 20 and 200) to be scheduled and the number of

machines (20) target of the scheduling. The GPU-based B&B has been implemented using C-CUDA 4.0, and compiled using *nvcc*. The experiments have been carried out on an Intel Xeon E5520 paired with a GPU device. E5520 is 64-bit and composed of two quad-core chips, and has a clock speed of 2.27GHz. The GPU device is an Nvidia Tesla C2050 with 448 CUDA cores (14 multiprocessors with 32 cores each), a clock speed of 1.15GHz, a 2.8GB global memory, a configurable shared memory (16 KB or 48 KB) and a warp size of 32.

In the following, an experimental study is presented with the objective to evaluate the performance impact of the GPU-based parallel evaluation of the lower bound, and the data access optimization. For each, we present the objectives of the experiments and report the obtained results. Two parameters are considered: the problem instances ( $n \times m$ ) (as rows in the tables and x-axis in the graphics) and the size of the pool of sub-problems to be evaluated (as columns in the tables and x-axis in the graphics). The first parameter gives information on the granularity of the thread computations. As the complexity of the computation of the lower bound is  $O(m^2.n.\log n)$ , for large problem instances (i.e. large values of  $n$  and  $m$ ) the grain size of the kernel executed by each thread is much higher. Moreover, the first parameter gives information on the size of the data structures to be mapped on the GPU memories. This is highly important for the study of the data access optimization approach. The second parameter is designated in the different experimental results by *pool size* (*block size*  $\times$  *number of threads/block*). This parameter is useful to get information on the time cost of the data transfer between CPU and GPU and on the total number of threads to be triggered on GPU.

For each pair of values associated to the two parameters, each table/graphics reports the corresponding parallel efficiency. Since the used instances are very hard to solve (optimal solutions for many of these instances are still not known), we used the approach defined in [11] to run experiments. Employing this method allows to obtain a random list  $L$  of subproblems such as the resolution of  $L$  lasts  $T_{cpu}$  minutes with a sequential B&B. To ensure that the subproblems explored by the GPU and CPU B&B versions are exactly the same, we initialize the pool of our GPU-based B&B with the same list  $L$  of subproblems used in the sequential version. If we suppose the resolution of the GPU-based B&B last  $T_{gpu}$  minutes, the parallel efficiency would be the ratio  $T_{cpu}/T_{gpu}$ : the execution time of the serial B&B on a single CPU core (without GPU) over the execution time of our GPU-based B&B on a CPU core coupled with a GPU device.

#### A. Performance impact of GPU-based parallelism

First, the objective of the experimental study presented in this section is to demonstrate that our GPU-based B&B allows one to significantly accelerate the resolution process whatever is the FSP instance. However, the best achieved acceleration depends strongly on the problem instance being solved and the size of the pool of sub-problems considered at execution. The second objective is therefore to exhibit the behavior of the

GPU acceleration according to the tackled problem instance and the considered pool size. More exactly, the goal is to find for each problem instance the best pool size required to maximize the benefit taken from the use of the GPU device.

The results reported in Table II are obtained without any data access optimization. The six matrices are generated on CPU and then copied to the GPU global memory. The size of the thread blocks is experimentally fixed to 256 threads. Average accelerations of  $\times 44,52$  to  $\times 60,64$  and picked at  $\times 77,46$  are achieved. In addition, the improvement of the parallel efficiency from a pool size of 4096 ( $16 \times 256$ ) to 8192 ( $32 \times 256$ ) is significant. The reason is that the number of blocks (16) for the first pool size is not sufficient to get a better acceleration. Indeed, it is known that the number of blocks must be fixed at least to the double ( $14 \times 2 = 28$  for the C2050 GPU card) of the number of multi-processors of the target GPU device. Furthermore, for  $50 \times 20$  and  $20 \times 20$  problem instances the best parallel efficiency is achieved for a pool size of 8192. For larger instances i.e.  $100 \times 20$  and  $200 \times 20$ , it is obtained with a pool size of 262144. These two pool size values correspond exactly to the two sizes of the pool for which the best ratio between lower bound evaluation time on CPU of the pool and its total communication time from CPU to GPU and from GPU to CPU.

#### B. Data access optimization

The objective is here to find the best mapping of the six data structures of the lower bound LB kernel on the memories of the GPU device. As quoted in Section III-B, such mapping depends on the sizes and access latencies/frequencies of these data structures and the GPU memories. The focus is put on the shared memory which is a key enabler for many high-performance CUDA applications. We also take care of adequately using the global memory by judiciously configuring the L1 cache that greatly enables improving performance over direct access to global memory. Indeed, the GPU device we are using in our experiments is a C2050 Tesla (see IV) which a device based on the NVIDIA Fermi architecture. In the Fermi architecture, each multiprocessor of the GPU device is provided with a 64 KB local storage that can be configurable into shared memory and L1 cache. For this reason and in order to achieve further performances, we divided the 64 KB memory according to the scenario we are experimenting. For the scenario where the data structures are put on the shared memory the 64 KB of available storage are split on 48 KB for shared memory and 16 KB for L1 cache. For the scenario where the data sets are put on global memory we used 16 KB for shared memory and 48 KB for L1 cache.

As far as the data structures of the lower bound function are concerned, their complexities in terms of size and access frequency are reported in Table I (see Section II-D). According to Table I,  $RM$ ,  $QM$  and  $MM$  have a small size, so their storage in the shared memory allows a very poor performance improvement. Therefore, whatever is the memory to which they are off-loaded, the performance impact is not significant. However, for large FSP instances (with  $n = 200$ ), the total

Problem instance	4096 16×256	8192 32×256	16384 64×256	32768 128×256	65536 256×256	131072 512×256	262144 1024×256
200×20	46,63	60,88	63,80	67,51	73,47	75,94	<b>77,46</b>
100×20	45,35	58,49	60,15	62,75	66,49	66,64	<b>67,01</b>
50×20	44,39	<b>58,30</b>	57,72	57,68	57,37	57,01	56,42
20×20	41,71	<b>50,28</b>	49,19	45,90	42,03	41,80	41,65
Average Speedup	44,52	56,99	57,72	58,46	59,84	60,35	60,64

TABLE II

PARALLEL EFFICIENCY FOR DIFFERENT PROBLEM INSTANCES AND POOL SIZES. ALL THE MATRICES  $JM$ ,  $PTM$ ,  $LM$ ,  $RM$ ,  $QM$  AND  $MM$  ARE LOCATED IN THE GPU GLOBAL MEMORY.

amount of memory required to store the other data structures i.e.  $JM$  and  $LM$  (38KB each) and  $PTM$  (4KB) is 80KB, which is greater than the available shared memory space (48KB). Therefore, only two of them can be put in the shared memory.  $LM$  has a double memory size than  $JM$ , and its access frequency is much lower, so it is better to map  $JM$  on the shared memory. Furthermore,  $PTM$  has the same access frequency than  $JM$  but requires less memory space. Consequently, the focus is put on the study of the performance impact of the placement of  $JM$  and  $PTM$  on the shared memory.  $PTM$  and  $JM$  are stored in shared memory and all others are placed on global memory.

Table III reports the behavior of the parallel efficiency averaged on the different problem instances (sizes) as a function of the pool size. The table shows that the parallel efficiency grows on average with the growing of the pool size in the same way as in Table II. For instance, for the largest problem instance and pool size, the parallel efficiency grows up to from  $\times 77,46$  ( $PTM$  and  $JM$  in global memory) to  $\times 100,48$  ( $PTM$  and  $JM$  in shared memory) (23%).

Figure 4 depicts the behavior of the parallel efficiency for the different problem instances (sizes). The pool size is fixed to 262144 ( $1024 \times 256$ ). According to the graphics, first, the efficiency is improved for all instances and the improvement is more significant for large problem instances. Second, the behavior of the efficiency improvement is not the same if shared memory is used or not. Indeed, according to the CUDA GPU occupancy calculator the size of the shared memory occupied by the data structures limits the number of active thread warps to 32 for  $20 \times 20$  and  $50 \times 20$  problem instances, and to 16 for  $100 \times 20$  and  $200 \times 20$  problem instances. When only global memory is used, the improvement is linear and the slope remains the same as the number of active thread warps remains the same (32) whatever is the problem instance. The only limiting factor of the active thread warps is the number of registers which is 26 in our case. In this case, the size of the occupied shared memory is lower and is not a limiting factor for the occupancy or number of active threads. On the other hand, when shared memory is used the slope of the efficiency improvement is much higher from  $20 \times 20$  to  $50 \times 20$  (small data structures) than from  $100 \times 20$  to  $200 \times 20$  (large data structures). The reason is that according to CUDA GPU occupancy calculator in addition to the number of registers the size of the occupied shared memory is also a limiting factor

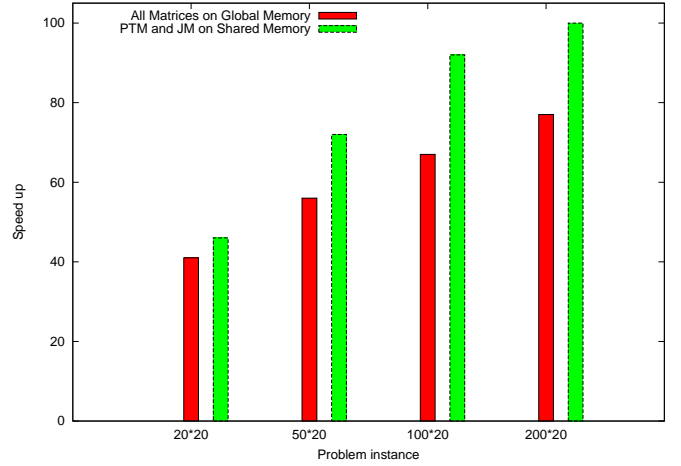


Fig. 4. Average parallel efficiency for different problem instances:  $PTM$  and  $JM$  are put together in the shared memory, the pool size is fixed to  $1024 \times 256$ .

of thread occupancy and thus parallel efficiency.

## V. PERFORMANCES COMPARISON WITH A MULTI-THREADED PARALLEL B&B ALGORITHMS

With the advent of multi-core processors and their promised enhancement in software development performances, the use of multi-core processors for designing parallel algorithms become highly widespread. Unlike distributed computing systems, one of the advantages of multi-core systems is the possibility to parallelize the algorithm using threads instead of processes. Indeed, while processes in the same machine have their own virtual memory, threads of a process share the same virtual memory which significantly impact the performances.

Several implementation of a multi-threaded B&B have been proposed in previous research works [10], [9], [15], [16]. These multi-threaded B&B algorithms can be classified into two categories: low and high-level. In a low-level multi-threaded B&B, a low-level thread model such as POSIX Threads is used [12], [9] while in a high-level multi-threaded B&B a high-level thread model such as OpenMP [2] is used.

In order to further evaluate the performances of the proposed GPU-based B&B algorithm, we compare it to a low-level multi-threaded B&B [9] designed on top of a multi-core system, using the POSIX Threads library.

Problem instance	4096 16×256	8192 32×256	16384 64×256	32768 128×256	65536 256×256	131072 512×256	262144 1024×256
200×20	66,13	87,34	88,861	95,23	98,83	99,89	<b>100,48</b>
100×20	65,85	86,33	87,60	89,18	91,41	92,02	<b>92,39</b>
50×20	64,91	<b>81,50</b>	78,02	74,16	73,83	73,25	72,71
20×20	53,64	<b>61,47</b>	59,55	51,39	47,40	46,53	46,37
Average Speedup	62,63	79,16	78,51	77,49	77,87	77,92	77,99

TABLE III

PARALLEL EFFICIENCY FOR DIFFERENT FSP INSTANCES AND POOL SIZES OBTAINED WITH DATA ACCESS OPTIMIZATION. *PTM* AND *JM* ARE PLACED TOGETHER IN SHARED MEMORY AND ALL OTHERS ARE PLACED IN GLOBAL MEMORY.

In order to perform a fair comparison with the obtained results of our GPU-based approach, the used multi core system must have the same computational power in term of theoretical peak of floating-point operations per second. The floating-point operations per second (FLOPS) is a common measure of a computer's performance, especially in fields of scientific calculations. Indeed, FLOPS is a good indicator to measure performance on digital signal processing, scientific simulations, etc. It is particularly used in supercomputer ratings, like TOP500 [22].

As quoted in IV, the experiments have been carried out on an Nvidia Tesla C2050. According to its constructor NVIDIA [18], the theoretical double precision floating-point performance peak of this GPU device is about 515 GFLOPS. For the multi-threaded version of the B&B we have carried out experimentation on an Intel Core i7-970 Processor which is 64-bit and composed of six physical cores and 12 threads [21] having each a theoretical double precision floating-point performance peak of 76.8 GFLOPS [20].

Table IV reports the speedup of the parallel multi-threaded B&B averaged on the different problem instances (sizes). The columns correspond to the number of parallel running B&B process and the corresponding theoretical peak of GFLOPS. The rows correspond to the problem instances defined by (Number of jobs × Number of machines). The same experimental protocol as the for GPU computation is used (see section IV). The reported speedups are calculated relatively to a serial B&B on a single CPU core. Results shows that the parallel efficiency grows on average with the growing of the number of computing core used. However, the improvement is not linear and the slop decrease as long as the number of the used computing core raises. This behavior might be due to the operating system which handles additional page faults and context switches when the number of threads increases.

Figure 5 shows the comparison between the obtained speedups with our GPU-based B&B and the multithreaded-based B&B. The speedups are calculated relatively to the same sequential version of the B&B algorithm. For a same computational power, our approach for designing B&B algorithms on top of GPU accelerators is much more efficient than the multi-threaded B&B whatever the instance is. Indeed, for a computational power around 500 GFLOPS, the acceleration calculated when using the GPU-based B&B for the instances 20 jobs over 20 machines is ×61,47. For the same category

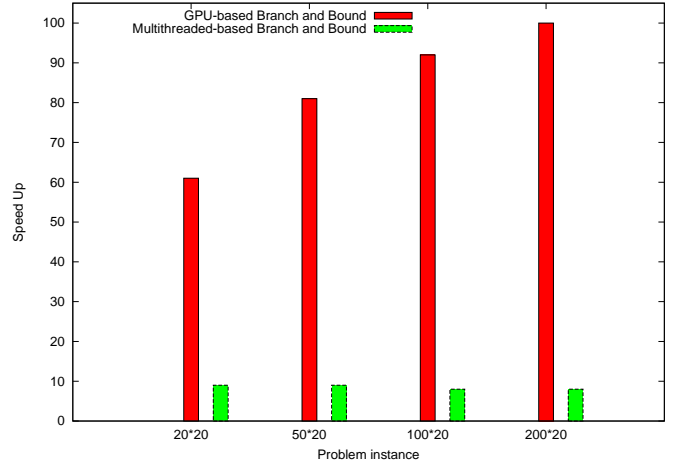


Fig. 5. Comparison between the average parallel efficiency for different problem instances obtained with a GPU and a multithreaded-based B&B for a same computational power (500 GFLOPS).

of instances (20 jobs over 20 machines) and a same computational power of 500 GFLOPS which corresponds to 7 CPU computing cores for the Intel Core i7-970 Processor, the speedup over a sequential version of the multi-threaded based B&B is ×9,22. Results show also that parallel efficiency for the GPU-based approach increases with the size of the problem being tackled while it is almost the same for the multi-threaded based algorithm. This is due to the complexity of the computation of the lower bound which is  $O(m^2 \cdot n \cdot \log n)$ . When the size of the problem instance (i.e. large values of  $n$  and  $m$ ) increases, the grain size of the kernel executed by each thread becomes higher which significantly increases the GPU throughput. For instance, for the problems of the category 200 jobs over 20 machines, the reported speedup of our approach is about ×100,48 while the speedup calculated for the multithreaded version is ×8,76 which corresponds to an improvement of ×11,47. Over all the experimented instance categories, the GPU-based B&B run faster than the multithreaded-based B&B.

## VI. CONCLUSION AND FUTURE WORK

In this paper, we have revisited the parallel B&B algorithm for solving permutation-based combinatorial optimization problems such as FSP on GPU accelerators. The contributions consist in proposing: (1) a GPU-based parallel design



Number of B&B Threads Theoretical Peak of GFLOPS	3	5	7	9	11
200×20	4,03	6,98	8,76	9,04	9,32
100×20	4,27	7,08	8,82	9,39	9,85
50×20	4,38	7,27	9,06	9,64	10,17
20×20	4,43	7,35	9,22	10,04	10,85

TABLE IV  
PARALLEL EFFICIENCY FOR DIFFERENT PROBLEM INSTANCES USING THE MULTI-THREADED BASED B&B.

and implementation of the parallel bounding model ; (2) a data access optimization approach to take into account the memory constraints of the GPU device. The Flow-Shop scheduling problem has been considered as a case study together with the Johnson's lower bound [5], extended in [3] to more than two machines. The proposed approaches have been experimented using a Tesla C2050 GPU card on 4 different classes of FSP instances.

In our proposed GPU-based approach, the decomposition and pruning of the sub-problems is performed on CPU and the evaluation of their lower bounds (bounding operation) is executed on GPU. Pools of sub-problems are off-loaded from CPU to GPU to be evaluated by blocks of threads. After evaluation, the lower bounds are returned back to the CPU. The experimental results show that accelerations up to  $\times 77$  can be obtained especially for large problem instances and large pools of sub-problems. As shown in the reported results the pool size that enables to achieve the best acceleration of the bounding mechanism depends strongly on the size of the problem instance being solved. Therefore, this parameter has to be determined at runtime by testing different pool sizes.

The proposed data access optimization is based on a preliminary analysis of the lower bound function. Such analysis allowed us to identify six data structures for which we have proposed a complexity analysis in terms of memory size and access frequency. Due to the limited size of the shared memory the matrices do not fit in all together. According to the complexity study, the recommendation is to put in the shared memory the Johnson's and the processing time matrices ( $JM$  and  $PTM$ ) if they fit in together. The other data structures are mapped to the global memory combined with the L1 cache (see IV-B). Such recommendation has been confirmed through extensive experiments using the Taillard's benchmarks of the Flow-Shop problem and a recent C2050 Tesla GPU card. The optimizations obtained with the proposed approaches allowed us to achieve accelerations up to  $\times 100$  compared to a single CPU-based B&B and up to  $\times 11$  compared to a multi-threaded CPU-based execution.

We are currently investigating the combination of the GPU-based bounding model with the multi-core parallel search tree exploration for the design and implementation of a GPU-accelerated multi-core B&B algorithm. In the near future, we plan to extend this work to a cluster of GPU-accelerated multi-core processors. From application point of view, the objective is to solve to optimality challenging difficult and

unsolved Flow-Shop instances as we did it for one  $50 \times 20$  problem instance using grid computing [11]. Finally, we plan to investigate other lower bound functions to deal with other combinatorial optimization problems.

## REFERENCES

- [1] B. Gendron and T.G. Crainic. Parallel Branch-and-Bound Algorithms: Survey and Synthesis. *Operations Research*, 42(06):1042–1066, 1994.
- [2] B. Chapman, G. Jost, and R. Van Der Pas. Using OpenMP: portable shared memory parallel programming. Volume 10. The MIT Press, 2007.
- [3] B. J. Lageweg, J. K. Lenstra and A. H. G. Rinnooy Kan. A general bounding scheme for the permutation flow-shop problem. *Operations Research*, 26(1):53–67, 1978.
- [4] M.R. Garey and D.S. Johnson. *Computers and Intractability: A Guide to the Theory of NP-Completeness*. W. H. Freeman & Co., New York, NY, 1979.
- [5] S.M. Johnson. Optimal two and three-stage production schedules with setup times included. *Naval Research Logistics Quarterly*, 1:61–68, 1954.
- [6] E. Taillard. Taillard's FSP benchmarks. <http://mistic.heig-vd.ch/taillard/problemes.dir/ordonnancement.dir/ordonnancement.html>.
- [7] S. Tschoke, R. Lubling and B. Monien. Solving the traveling salesman problem with a distributed branch-and-bound algorithm on a 1024 processor network. In *Proc. of 9<sup>th</sup> Intl. Parallel Processing Symposium (IPPS)*, pp. 182 - 189, 1995.
- [8] R. Allen, L. Cinque, S. Tanimoto, L. Shapiro and D. Yasuda. A parallel algorithm for graph matching and its MasPar implementation. *IEEE Transactions on Parallel and Distributed Systems*, Vol. 8, No. 5, 1997.
- [9] L.G. Casadoa, J.A. Martneza, I. Garcaa and E.M.T. Hendrixb. Branch-and-Bound interval global optimization on shared memory multiprocessors. *Optimization Methods and Software*, Vol. 23, No.5, pp. 689–701, 2008.
- [10] L. Barreto and M. Bauer. Parallel Branch and Bound Algorithm-A comparison between serial, OpenMP and MPI implementations. *Journal of Physics: Conference Series*, Vol. 256, No.5, pp. 012018, 2010.
- [11] M. Mezma, N. Melab and E-G. Talbi. A Grid-enabled Branch and Bound Algorithm for Solving Challenging Combinatorial Optimization Problems. In *Proc. of 21th IEEE Intl. Parallel and Distributed Processing Symp. (IPDPS)*, Long Beach, California, March 26th–30th, 2007.
- [12] B. Nichols, D. Buttlar, and J.P. Farrell. *Pthreads programming*. O'Reilly Media, 1996.
- [13] M. Djamai, B. Derbel and N. Melab. Distributed B&B: A Pure Peer-to-Peer Approach. In *Proc. of IEEE IPDPS'2011, Woks. on Large-Scale Parallel Processing (LSPP)*, May 16–20, Anchorage (Alaska), 2011.
- [14] T-V. Luong, N. Melab and E-G. Talbi. GPU Computing for Parallel Local Search Metaheuristic Algorithms. *IEEE Transactions on Computers*, <http://doi.ieeecomputersociety.org/10.1109/TC.2011.206>, 2012.
- [15] R. Paulavičius and J. Žilinskas. Parallel branch and bound algorithm with combination of Lipschitz bounds over multidimensional simplices for multicore computers. *Parallel Scientific Computing and Optimization*, Springer, pages 93–102, 2009.
- [16] JF. Sanjuan-Estrada, LG. Casado and I. García. Adaptive parallel interval branch and bound algorithms based on their performance for multicore architectures, *The Journal of Supercomputing*, Springer, pages 1–9, 2011.
- [17] NVIDIA. CUDA C Programming Best Practices Guide. [http://developer.download.nvidia.com/compute/cuda/2\\_3/toolkit/docs/NVIDIA\\_CUDA\\_BestPracticesGuide\\_2.3.pdf](http://developer.download.nvidia.com/compute/cuda/2_3/toolkit/docs/NVIDIA_CUDA_BestPracticesGuide_2.3.pdf).
- [18] [http://www.nvidia.com/docs/IO/43395/NV\\_DS\\_Tesla\\_C2050\\_C2070\\_jul10\\_lores.pdf](http://www.nvidia.com/docs/IO/43395/NV_DS_Tesla_C2050_C2070_jul10_lores.pdf)
- [19] [http://en.wikipedia.org/wiki/Comparison\\_of\\_Nvidia\\_graphics\\_processing\\_units](http://en.wikipedia.org/wiki/Comparison_of_Nvidia_graphics_processing_units)
- [20] [http://download.intel.com/support/processors/corei7/sb/core\\_i7-900\\_d.pdf](http://download.intel.com/support/processors/corei7/sb/core_i7-900_d.pdf)
- [21] [http://ark.intel.com/products/47933/Intel-Core-i7-970-Processor-%2812M-Cache-3\\_20-GHz-4\\_80-GTs-Intel-QPI%29](http://ark.intel.com/products/47933/Intel-Core-i7-970-Processor-%2812M-Cache-3_20-GHz-4_80-GTs-Intel-QPI%29)
- [22] <http://www.top500.org/>